Multidrug-resistant cancer cells contain two populations of P-glycoprotein with differently stimulated P-gp ATPase activities: evidence from atomic force microscopy and biochemical analysis

Stéphane BARAKAT*, Landry GAYET*, Guila DAYAN*, Stéphane LABIALLE†, Adina LAZAR‡, Vladimir OLEINIKOV§, Anthony W. COLEMAN‡ and Loris G. BAGGETTO*[1]

*Thérapie transcriptionnelle des cellules cancéreuses, IBCP - UMR 5086 CNRS UCBL, 7 Passage du Vercors, 69367 Lyon cedex 07, France, †McGill University, Royal Victoria Hospital, F3.32, 687 Pine avenue West, Montreal, QC, Canada H3A 1A1, ‡Assemblages moléculaires d'intérêt biologique, IBCP - UMR 5086 CNRS UCBL, 7 Passage du Vercors, 69367 Lyon cedex 07, France, and §Shemyakin and Ovchinnikov Institute of Bioorganic Chemistry, Russian Academy of Sciences, Miklukho-Maklaya 16/10, Moscow B-437, GSP 117997, Russia

Considerable interest exists about the localization of P-gp (P-glycoprotein) in DRMs (detergent-resistant membranes) of multidrug resistant cancer cells, in particular concerning the potential modulating role of the closely related lipids and proteins on P-gp activity. Our observation of the opposite effect of verapamil on P-gp ATPase activity from DRM and solubilized-membrane fractions of CEM-resistant leukaemia cells, and results from Langmuir experiments on membrane monolayers from resistant CEM cells, strongly suggest that two functional populations of P-gp exist. The first is located in DRM regions: it displays its optimal P-gp ATPase activity, which is almost completely inhibited by orthovanadate and activated by verapamil. The second is located elsewhere in the membrane; it displays a lower P-gp ATPase activity that is less sensitive to orthovanadate and is inhibited by verapamil. A 40 % cholesterol depletion of DRM caused the loss of 52 % of the P-gp ATPase activity. Cholesterol repletion allowed recovery of the initial P-gp ATPase activity. In contrast, in the solubilized-membrane-containing fractions, cholesterol depletion and repletion had no effect on the P-gp ATPase activity whereas up to 100 % saturation with cholesterol induced a 58 % increased P-gp ATPase activity, while no significant modification was observed for the DRM-enriched fraction. DRMs were analysed by atomic force microscopy: 40–60 % cholesterol depletion was necessary to remove P-gp from DRMs. In conclusion, P-gp in DRMs appears to contain closely surrounding cholesterol that can stimulate P-gp ATPase activity to its optimal value, whereas cholesterol in the second population seems deprived of this function.

Key words: atomic force microscopy, ATPase, caveolin-1, detergent-resistant membranes, multidrug resistance, P-glycoprotein.

INTRODUCTION

The failure of cancer chemotherapy is mainly due to the development of the MDR (multidrug resistance) phenotype. Typical MDR is characterized by overexpression of membrane transporters. Among the most studied, P-gp (P-glycoprotein) is a 170 kDa glycoprotein, which belongs to the superfamily of ABC (ATP-binding-cassette) transporters [1]. Such proteins can actively translocate a wide variety of lipophilic chemotherapeutic agents across the membrane on ATP hydrolysis [2], thus decreasing their intracytoplasmic concentrations below cytotoxic levels.

P-gp has been localized in caveolae of sensitive AuxB1 and resistant CH(R)C5 cells as well as in brain capillaries [3]. Caveolae are small flask-shaped invaginated membranes present in many cell types. They are enriched with glycosphingolipids, cholesterol and sphingomyelin [4,5]. The process of invagination requires the presence of cholesterol and caveolin-1 [6], two major components of caveolae [7]. Caveolae and microdomains are tightly packed in a highly structured, liquid-ordered state [8]. These characteristics account for the resistance of microdomains to solubilization by cold, non-ionic detergents, thus defining DRMs (detergent-resistant membranes) [9].

Previous observations suggested that overall changes in the structural organization of plasma membranes from chemo-resistant lymphoblastic leukaemia cells are related to the acquisition of the MDR phenotype [10,11]. Furthermore, in some cases, the MDR phenotype has been linked to increased amounts of cholesterol, sphingomyelin, glucosylceramide, caveolin-1 and caveolae [12]. Moreover, it has been shown that P-gp interacts with a variety of lipids (such as phosphatidylethanolamine and phosphatidylserine) that are capable of modulating its activity [13,14]. Thus in this regard, P-gp has been reconstituted into a mixture of phosphatidylcholine and phosphatidic acid, thereby promoting P-gp ATPase activity [15]. Likewise, stimulation or inhibition of the P-gp ATPase activity by drugs may be affected by lipids, such as cholesterol, surrounding the transporter [16]. Recently, P-gp has been localized in non-caveolar DRMs and other ABC transporters like MRP1 have been localized in caveolae-containing DRMs [17]. Furthermore, the transport activity of P-gp may be modulated by its interaction with caveolin-1 [18], thus providing more information about the involvement of DRMs, and particularly caveolae, in the MDR phenotype.

Cholesterol is involved in both P-gp ATPase and transport activities [18]. Cholesterol depletion by MβCD (methyl-β-cyclodextrin) does not affect the rhodamine 123 transport activity whereas the P-gp ATPase activity is lost [19]. However, certain details of this work have not been documented such as the location of active P-gp in cells and the localization of cholesterol that modulates the P-gp ATPase activity in membrane subfractions. It has been reported that P-gp is mostly localized in the cholesterol-rich DRM regions of the plasma membrane; however, other studies showed that P-gp and cholesterol could also be found

Abbreviations used: ABC, ATP binding cassette; AFM, atomic force microscopy; DRM, detergent-resistant membrane; MDR, multidrug resistance; MβCD, methyl-β-cyclodextrin; P-gp, P-glycoprotein.

[1] To whom correspondence should be addressed (email lg.baggetto@ibcp.fr).

elsewhere, depending on the method used to extract DRMs [17,20,21]. Several membrane preparations such as whole plasma membrane [13], liposomes containing reconstituted P-gp [22] and membrane vesicles [16] have been used to show that cholesterol was capable of modulating the P-gp ATPase activity. However, the results obtained did not provide any evidence about the localization of active P-gp (in terms of P-gp ATPase activity) in particular membrane regions, neither did the results provide information concerning the stimulation of P-gp ATPase activity by cholesterol that belonged to DRMs or to other membrane regions.

Since P-gp may be present in any region of the plasma membrane and because of the particular cholesterol and other lipid compositions found in MDR cells, we examined the distribution of the P-gp ATPase activity in solubilized-membrane- and DRM-containing fractions and established a direct relationship between specific membrane regions and stimulated P-gp ATPase activity. In addition, we showed that most of the cholesterol involved in the P-gp ATPase activity belonged to DRM regions, thereby defining two P-gp populations that could be distinguished by the presence or absence of closely surrounding cholesterol. Finally, we visualized by AFM (atomic force microscopy), the effects of cholesterol depletion and repletion on the structure of the membranes in the DRM-containing fraction, a study that has never been previously reported for biological membranes.

MATERIALS AND METHODS

Chemicals

All products, unless otherwise indicated, were from Sigma–Aldrich (L'Isle-d'Abeau Chesnes, France). Muscovite mica was from Goodfellow SARL (Lille, France).

Cell culture

Human CEM acute lymphoblastic leukaemia cells were grown in RPMI 1640 medium supplemented with 10 % (v/v) fetal bovine serum, 100 units/ml penicillin, 100 μg/ml streptomycin and 0.25 μg/ml amphotericin B at 37 °C in a water-saturated atmosphere under 5 % CO_2. The drug-resistant cell lines, CEM/VLB0.45 and CEM/VLB5, were established by growing the corresponding sensitive parental CEM cell line (CEM/S) in a medium containing stepwise-increasing concentrations of vinblastine for 24 months [23]. CEM/VLB0.45 and CEM/VLB5 cells were grown in the presence of 0.45 and 5 μg/ml of vinblastine respectively.

Isolation of DRMs

All steps were performed at 4 °C. Caveolin-1-enriched membrane domains were purified from cultured CEM/S, CEM/VLB0.45 and CEM/VLB5 cells as described in [9] and modified as follows. Cells (1.3×10^8) were suspended in 330 μl of Mes buffer (25 mM 2-*N*-morpholino-ethane sulphonic acid, pH 6.5, 0.15 M NaCl, 2 mM phenylmethyl sulphonyl fluoride, 1 μM leupeptin and 2 μM pepstatin A) and homogenized by sonication with three 30 s bursts separated by a 1 min cooling period (micro-probe Branson sonicator). Triton X-100 and sucrose concentrations were adjusted to 1 and 40 % respectively by the addition of 330 μl of 2 % (w/v) Triton X-100 and 660 μl of 80 % (w/v) sucrose, both prepared in Mes buffer. Extracts were homogenized by pipetting and placed at the bottom of an ultracentrifuge tube. A 5–25 % discontinuous sucrose gradient was placed above by successive additions of 830 μl of 25 % sucrose, 830 μl of 15 % sucrose and 830 μl of 5 % sucrose, prepared in Mes buffer, followed by centrifugation at 100 000 ***g*** for 18 h at 4 °C in a swinging Beckman SW60Ti rotor. A milky light-scattering band corresponding to DRMs was confined to the 15–25 % sucrose interface. From the top of each gradient, a total of seven fractions (500, 500, 750, 500, 750 and 1000 μl, and the last one containing the pellet) were collected and named F1–F7 respectively. Each fraction was then resuspended in a final volume of 4 ml of 10 mM Tris/HCl (pH 7.4) and centrifuged at 100 000 ***g*** for 1 h at 4 °C, followed by removal of supernatant. For comparability, each pellet was homogenized with a piston-pellet in 200 μl of 0.25 M sucrose and 10 mM Tris/HCl (pH 7.4). The DRM preparation from each cell type (CEM/S, CEM/VLB0.45 and CEM/VLB5) was used for ATPase activity assays, SDS/PAGE (10 % polyacrylamide) and immunoblot analyses.

Cholesterol depletion and repletion in the DRM-enriched fraction

After DRM extraction, fractions F3 and F7 were subdivided into two aliquots and one of them was incubated with 1.5 mM MβCD during 90–120 min at 37 °C followed by centrifugation at 100 000 ***g*** (1 h and 4 °C). Membrane repletion of cholesterol was realized by incubating an aliquot of previously depleted DRMs with cholesterol-loaded MβCD (6.5 mM cholesterol and 66.7 mM MβCD) for 90–120 min at 37 °C. Cholesterol saturation was realized in the same way on the non-treated F3 and F7 fractions. The reaction was followed by a centrifugation at 100 000 ***g*** for 1 h at 4 °C. The pellets from depleted, non-depleted, repleted and saturated F3 or F7 aliquots were resuspended in 50 μl of 10 mM Tris/HCl and 0.25 M sucrose (pH 7.4). Protein, total cholesterol and ATPase activity were measured as described below.

Measurement of P-gp ATPase activity

ATP hydrolysis by P-gp was measured using an NADH fluorometric assay (SLM Aminco spectrofluorimeter) as described previously [15]. To 1–10 μl of each fraction, 0, 200 or 400 μM orthovanadate was added. Variable concentrations of verapamil (0–1060 μM) were added to DRM-containing fractions and solubilized-membrane fractions. P-gp ATPase activity was assayed after the addition of a non-P-gp ATPase inhibitor mixture (20 mM NaN_3, 1 mM EGTA, 4 mM ouabain and 1 μg/ml oligomycin) to the assay medium. For each assay, the basic ATPase activity of each fraction from the CEM/S cells was taken as a control.

Protein and cholesterol quantification

Total protein concentration was measured by the Bradford method [24] (Bradford reagent; Sigma) using BSA as standard. Cholesterol extraction from cell membranes was performed as described in [25]. Total membrane cholesterol contents were measured using the CHOD-PAP reagents (BIOLABO, Les Hautes Rives, France) according to [26]. The method had previously been validated for this application [27].

Electrophoresis and immunoblotting experiments

SDS/PAGE of all fractions was performed on 8 and 12.5 % polyacrylamide gels containing 1 % 2-mercaptoethanol and 0.1 % SDS at 110 V, at room temperature for 1.5 h. Gels were transferred on to a 0.45 μm BA85 nitrocellulose membrane (Schleicher and Schüell, Elquevilly, France) and then blotted with C219 anti-P-gp (Dako, Carpinteria, CA, U.S.A.; dilution 1:500) or anti-caveolin-1 (Transduction Laboratories, Interchim, France; dilution 1:100) monoclonal antibodies. Bands were visualized using an alkaline phosphatase-labelled antibody (Sigma), in the presence of

5-bromo-4-chloro-3-indolyl phosphate and Nitro Blue Tetrazolium chloride.

Langmuir compression isotherms

The effect of P-gp on the properties of monolayers prepared from P-gp-containing plasma membrane preparations of CEM/VLB0.45 cells as described in [15], in the absence or presence of different amounts of verapamil as indicated below, was analysed by the Langmuir method as described previously [28]. To study the effect of verapamil on P-gp-containing monolayers, a calculated amount of verapamil was introduced into the subphase. The monolayer was maintained for approx. 10 min and was then compressed at a constant rate of 20 cm^2/min by the movable barrier; isotherms of the surface pressure π and the surface potential $\Delta\psi$ were recorded simultaneously as a function of monolayer area A for a known amount of the protein in the monolayer. The dependence of the surface potential on the surface area induces a jump of potential caused by the orientation of lipid molecules. Since the difference between the area at which the surface potential jump $A_{\Delta\psi}$ occurs and the area at which the surface pressure A_π starts increasing is indicative of the nature of lipids weakly bonded to proteins, this was used to estimate the stability of lipid–protein complexes.

AFM imaging

Measurements by AFM were performed using a Thermomicroscope Explorer system equipped with a 100 μm scanner, in the non-contact mode. The scanning speed was 1 Hz and the resolution 500 × 500. For each sample, the scanning was realized at a scan size of 25 μm × 25 μm. Cantilevers used were silicon, the resonance frequency was $f_0 = 260$ kHz and the force constant was 45 N. Roughness analysis was performed using the area analysis subroutine of the SPML5 software program. The RMS (root-mean-squared roughness) area was defined as the square of the mean value of the square of the distance of the point (Z) from the image mean value (Z_i):

$$R_{\mathrm{ms}} = \sqrt{\frac{1}{N}\sum_{\mathrm{i}}(Z_{\mathrm{i}} - Z)^2} \quad (1)$$

All images are shown as shaded. F3 fractions, which were either cholesterol-depleted (40 and 60 %) or repleted, or either intact, were solubilized in 10 mM Tris/HCl (pH 7.4) and sonicated with the microprobe of a Branson sonicator for 3 × 30 s separated by a 30 s cooling period. Sonicated solution (5 μl) containing 1–2.5 μg of total proteins was deposited on to freshly cleaved mica. To eliminate salts, one rinsing was performed with 50 μl of distilled water, followed by overnight evaporation of the liquid at 20 °C.

RESULTS

Distribution of membrane cholesterol and P-gp in different membrane regions

Membranes from highly resistant CEM/VLB5 cells were purified and fractionated in a sucrose gradient in the presence of detergents to give seven fractions. After a second centrifugation to pellet the membranes, the supernatant was concentrated by Centriprep and Centricon concentrators and analysed by Western blot, which revealed that no remaining P-gp could be detected (results not shown). It is known that DRMs contain a large amount of cholesterol and that caveolin-1 is a specific marker of caveolae [29]. To validate the modified DRM purification method used, we

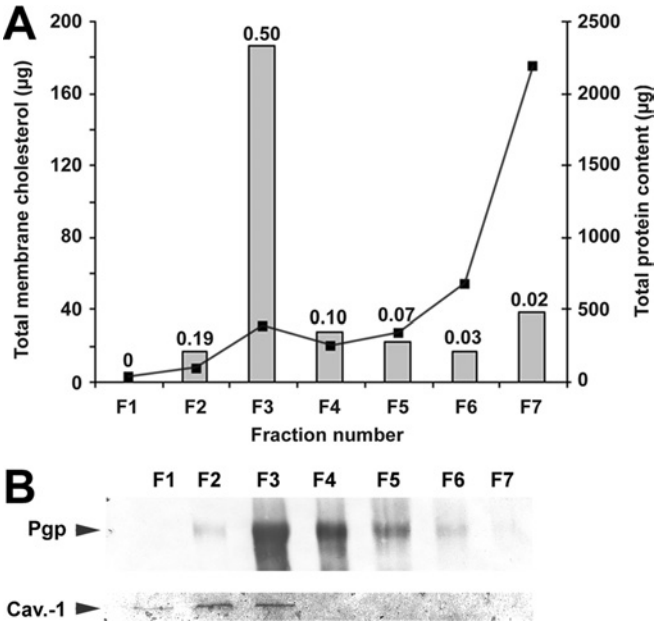

Figure 1 Distribution of total cholesterol from CEM/VLB5 cell membranes among the seven fractions resulting from the isolation procedure and P-gp localization of DRMs

Membrane fractionation was performed as described in the Materials and methods section. (**A**) Proteins (curve) and total cholesterol (bars) contents of each fraction of equal volume were measured as described in the Materials and methods section. Numbers above the bars represent the membrane cholesterol/total protein ratio (mg/mg). (**B**) Immunoblot of P-gp (upper row) and caveolin-1 (lower row) after electrotransfer of 10 and 40 μg of proteins respectively from each CEM/VLB5 membrane fraction, as described in the Materials and methods section. One typical result from duplicate experiments is presented.

measured the amount of total cholesterol in each fraction and detected the presence of caveolin-1 by immunoblotting. Figure 1(A) shows that the highest membrane cholesterol/total protein ratio (0.5 mg/mg) was localized to the milky fraction F3, which is classically reported to contain DRMs, whereas the cholesterol/total protein ratio in fraction F6 or F7 is much lower. Fraction F3 contained 60 % of the total amount of membrane cholesterol whereas fractions F6 and F7 contained 6 and 13 % of the total cholesterol amount respectively. Fraction F7, which contained solubilized membranes, displayed a cholesterol/total protein ratio of only 0.02, suggesting that cholesterol was particularly enriched in the protein environment of fraction F3. Besides, caveolin-1 was found in fractions F1–F3 (Figure 1B). The large amounts of cholesterol and caveolin-1 in fraction F3 showed the efficiency of the modified DRM extraction method.

As revealed by immunoblotting (Figure 1B), P-gp was enriched in both F3 and F4 fractions, where it was co-located with caveolin-1. P-gp was also present in the F7 fraction but at a barely detectable level. We therefore conclude that F3 is the fraction that contains the richest amounts of both DRMs and P-gp.

Distribution of the P-gp ATPase activity in different membrane fractions

The ATPase activity of P-gp was measured in each membrane fraction from the moderately chemoresistant CEM/VLB0.45 and the highly chemoresistant CEM/VLB5 cells. Total initial P-gp ATPase activity in membranes of CEM/VLB5 cell lysates was 129 nmol ATP/min; after the separation of membrane fractions, total P-gp ATPase activity recovered from all fractions from the same cells was 108 nmol ATP/min, corresponding to an 84 %

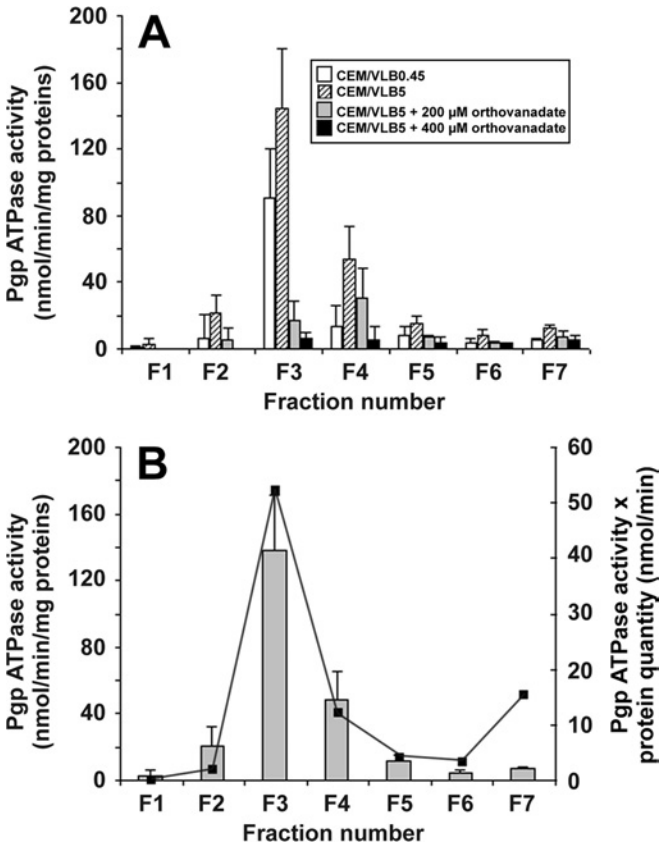

Figure 2 Effect of increasing concentrations of orthovanadate on the P-gp ATPase activity (A) and distribution of the P-gp ATPase activity (B) in different membrane fractions from CEM/VLB5 cells

Membrane fractionation and measurement of P-gp ATPase activity was performed as described in the Materials and methods section. (**A**) P-gp ATPase activity from CEM/VLB0.45 cell membranes (open bars) and CEM/VLB5 cell membranes in the absence (hatched bars) or presence of 200 μM (grey bars) or 400 μM (black bars) orthovanadate. Results are expressed as means $\pm$ S.D. of duplicates for four independent experiments for CEM/VLB5 cells and for three independent experiments for CEM/VLB0.45 cells. (**B**) The reported P-gp ATPase activity is a result of the difference between activities measured in the presence and absence of 400 μM orthovanadate (bars). For each fraction, P-gp ATPase activity was normalized to total protein content of the fraction (secondary *y* axis and line). Results are expressed as means $\pm$ S.D. of duplicates for four independent experiments (bars). One typical result from duplicate experiments is presented (line).

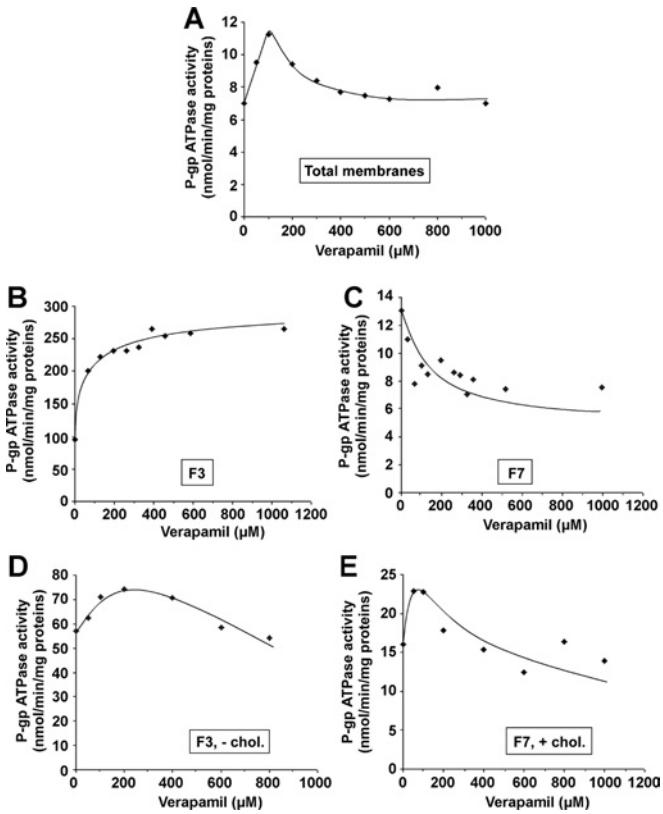

Figure 3 Verapamil-induced modulation of P-gp ATPase activity in the submembrane fractions from resistant CEM/VLB5 cells

P-gp ATPase activity was measured as described in the Materials and methods section in whole cell lysates (**A**), DRM-containing F3 (**B**), solubilized-membrane-containing F7 (**C**), 40 % cholesterol depleted F3 (**D**) and 104 % cholesterol saturated F7 (**E**) fractions. Data represent means of duplicate experiments; one typical experiment is presented.

activity recovery, and, as mentioned above, no quantifiable P-gp was lost during DRM purification. Figure 2(A) shows that the distribution of P-gp ATPase activity in the fractions from cells with the lowest resistance level (CEM/VLB0.45) strictly followed that of CEM/VLB5 cells. In both cases, the maximum P-gp ATPase activity was present in the DRM-containing fraction F3. Most of the remaining P-gp ATPase activity was present in fractions F2, F4 and F5. In addition, when the fraction F2, which contained contaminating DRMs, is compared with the fraction F6 containing contaminating solubilized membranes, P-gp quantities were almost identical (Figure 1B), but P-gp ATPase activity in fraction F2 was 2.75 times higher than that of the fraction F6 (Figure 2A), corroborating the fact that the most increased P-gp ATPase activity is located in the DRM-containing fraction.

To specifically identify typical P-gp ATPase activity in the different membrane fractions, we used orthovanadate and verapamil, two agents known respectively to specifically inhibit or activate P-gp ATPase. When the DRM-containing fraction F3 from CEM/VLB5 cells was considered, Figure 2(A) shows that the initial P-gp ATPase activity of 144.5 nmol $\cdot$ min^{-1} $\cdot$ (mg of total protein)$^{-1}$ was inhibited by 88.3 % in the presence of 200 μM orthovanadate and by 95.4 % in the presence of 400 μM orthovanadate. In contrast, when the soluble membrane-containing fraction F7 was considered, the initial P-gp ATPase activity of 12.2 nmol $\cdot$ min^{-1} $\cdot$ (mg of total protein)$^{-1}$ was inhibited by 37.8 % in the presence of 200 μM orthovanadate and by 57.7 % in the presence of 400 μM orthovanadate. The inhibition of P-gp ATPase activity by orthovanadate in fraction F7 suggested that P-gp was present in this fraction in amounts too low to be significantly detected by immunolabelling under our conditions.

No further inhibition of P-gp ATPase activity was observed for concentrations of orthovanadate above 400 μM. At this inhibitor concentration, Figure 2(B) shows that the highest P-gp ATPase activity was localized to the fraction F3, even when the high protein content of fraction F7 was taken into account (represented by the curve), suggesting that P-gp with the highest P-gp ATPase activity was found mostly in DRMs.

The effect of verapamil was assayed on a total membrane sample (Figure 3A) and on the two most representative membrane populations, i.e. DRM-containing fraction F3 (Figure 3B) and soluble membrane-containing fraction F7 (Figure 3C) from CEM/VLB5 cells. Figure 3(A) shows that treatment of CEM/VLB5 total membranes with increasing verapamil concentrations induced an activation that reached a maximal value in the presence of 75 μM verapamil, which is followed by an inhibition of the P-gp ATPase activity, in accordance with previously reported

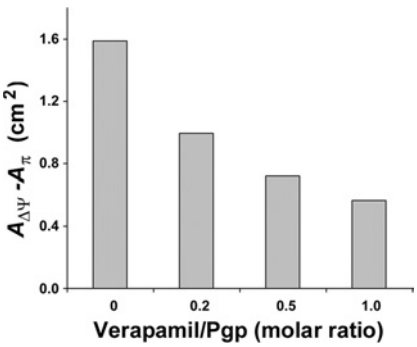

Figure 4 Effect of verapamil on the molecular organization of proteo-lipidic bilayers from CEM/VLB0.45 cell membranes examined by the Langmuir method

The difference between the area per lipid molecule without constraint at the moment when the electrostatic potential jump $A_{\Delta\psi}$ occurs and the area per lipid at the moment when the surface pressure A_π starts to rise is presented as a function of the molar ratio of verapamil per P-gp. The difference is representative of the $A_{\Delta\psi} - A_\pi$ difference, as described in the Materials and methods section. Since P-gp represents 11 % of total membrane protein in CEM/VLB0.45 cells [15] and since we consider that the molecular mass of P-gp equals 170 kDa, a verapamil/P-gp molar ratio of 1 corresponds to 2.9×10^{-3} mg of verapamil/mg of P-gp. Data represent means of duplicate experiments; one typical experiment is presented.

results by us [15] and others [30]. Figure 3(B) shows that increasing verapamil concentrations induced a 278 % activation of the initial P-gp ATPase activity in fraction F3 according to a hyperbolic curve, which reached a plateau at a verapamil concentration of approx. 100 μM. Conversely, in the F7 fraction, increasing verapamil concentrations induced a 50 % inhibition of P-gp ATPase activity according to a hyperbolic curve, which reached a plateau at approximately the same 100 μM verapamil concentration (Figure 3C). However, in that fraction, the P-gp ATPase activity in the absence of verapamil was 3.3 times lower than that measured in the F3 fraction because of the low P-gp/total protein ratio compared with that of fraction F3. To show how cholesterol could affect the P-gp ATPase activity in both DRM- and soluble membrane-containing fractions in the presence of verapamil, cholesterol was depleted from the previously enriched fraction F3 (Figure 3D), whereas the previously untreated fraction F7 was saturated with cholesterol (Figure 3E). In both cases, i.e. approx. 40 % cholesterol depletion of fraction F3 (Figure 3D) and approx. 100 % cholesterol saturation of fraction F7 (Figure 3E), the curves obtained tend to approach the biphasic curve observed with the total membrane fraction (Figure 3A). In the case of the DRM-enriched fraction in the absence of verapamil, cholesterol depletion caused a decreased P-gp ATPase activity (Figure 3D) when compared with that of the non-depleted fraction (Figure 3B). P-gp ATPase activity reached a maximum value of 74.3 nmol ATP $\cdot$ min^{-1} $\cdot$ (mg of protein)$^{-1}$ in the presence of 200 μM verapamil before decreasing steadily at higher verapamil concentrations (Figure 3D). In the cholesterol-saturated fraction F7, P-gp ATPase activity reached a maximum value of 22.8 nmol ATP $\cdot$ min^{-1} $\cdot$ (mg of protein)$^{-1}$ in the presence of approx. 75 μM verapamil and regularly decreased at higher verapamil concentrations (Figure 3E). However, in the absence of verapamil, cholesterol enrichment induced a higher P-gp ATPase activity compared with that obtained for the untreated fraction F7 (Figure 3C).

Due to the unexpected opposite effects of verapamil on the P-gp ATPase activity (Figures 3B and 3C) and the observation that cholesterol affects this activity, we measured the effect of verapamil on the properties of membrane monolayers from CEM/VLB0.45 cells by the Langmuir method. Figure 4 shows that

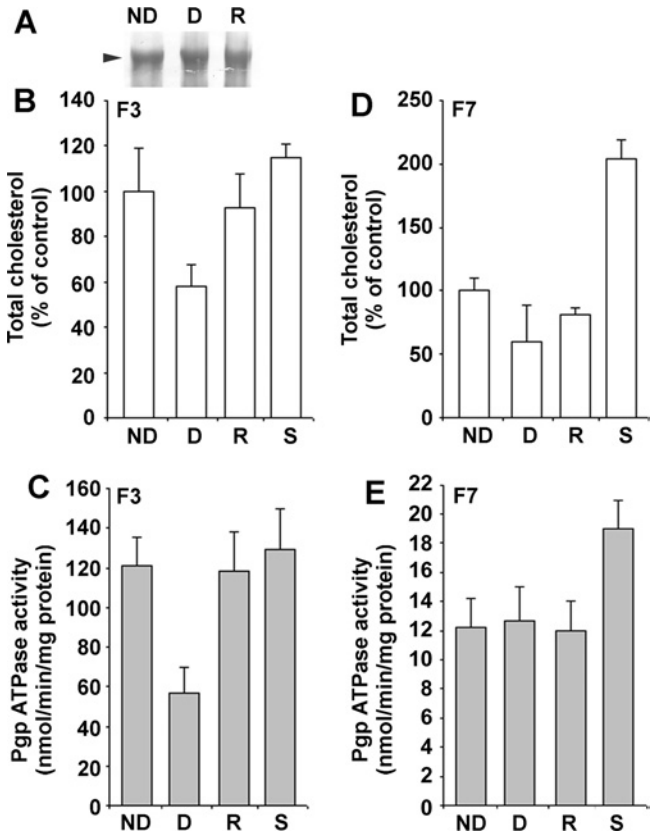

Figure 5 Cholesterol-induced modulation of the P-gp ATPase activity in P-gp from DRM-containing and solubilized-membrane-containing fractions

(**A**) P-gp was revealed by Western blot using the anti-P-gp C219 monoclonal antibody. Total proteins (10 μg) from F3, cholesterol-depleted F3 and cholesterol-repleted F3 fractions were deposited. Experimental conditions were identical for both cholesterol-depleted and cholesterol-saturated fractions. Cholesterol content in respectively F3 (**B**) and F7 (**D**) fractions after no treatment (ND), cholesterol depletion (D), cholesterol repletion (R) and saturation (S) of cholesterol. P-gp ATPase activity in respectively F3 (**C**) and F7 (**E**) fractions after no treatment, depletion, repletion and saturation of cholesterol. Experimental conditions are described in the Materials and methods section. Data represent means of triplicate experiments.

when the verapamil/P-gp molar ratio was increased, the $A_{\Delta\psi} - A_\pi$ difference decreased to a minimum value of 0.57 for a molar ratio of 1, according to a nonlinear relationship. This suggests that verapamil exerts a stabilizing action on the lipid–P-gp complex.

All these results suggest the existence of two P-gp populations, and the presence of cholesterol appears to be a good candidate to differentiate between them.

Modulation of P-gp ATPase activity by cholesterol in DRM-enriched and in solubilized membrane-enriched fractions

To characterize more precisely the P-gp ATPase activity in fractions F3 and F7, cholesterol was either removed or added from both fractions by using MβCD and MβCD-cholesterol respectively. To verify that no P-gp was extracted during cholesterol manipulation, a Western blot was performed. Figure 5(A) shows that P-gp quantities were identical in all treated or untreated fractions, suggesting that no preferential extraction of P-gp occurred during the depletion process compared with other proteins. P-gp ATPase activity was measured in non-depleted, depleted, repleted and saturated F3 and F7 fractions. MβCD treatment induced a depletion of 40 % cholesterol in the DRM-enriched fraction F3 (Figure 5B), in which the P-gp ATPase activity decreased to 57 nmol ATP $\cdot$ min^{-1} $\cdot$ (mg of total protein)$^{-1}$, which,

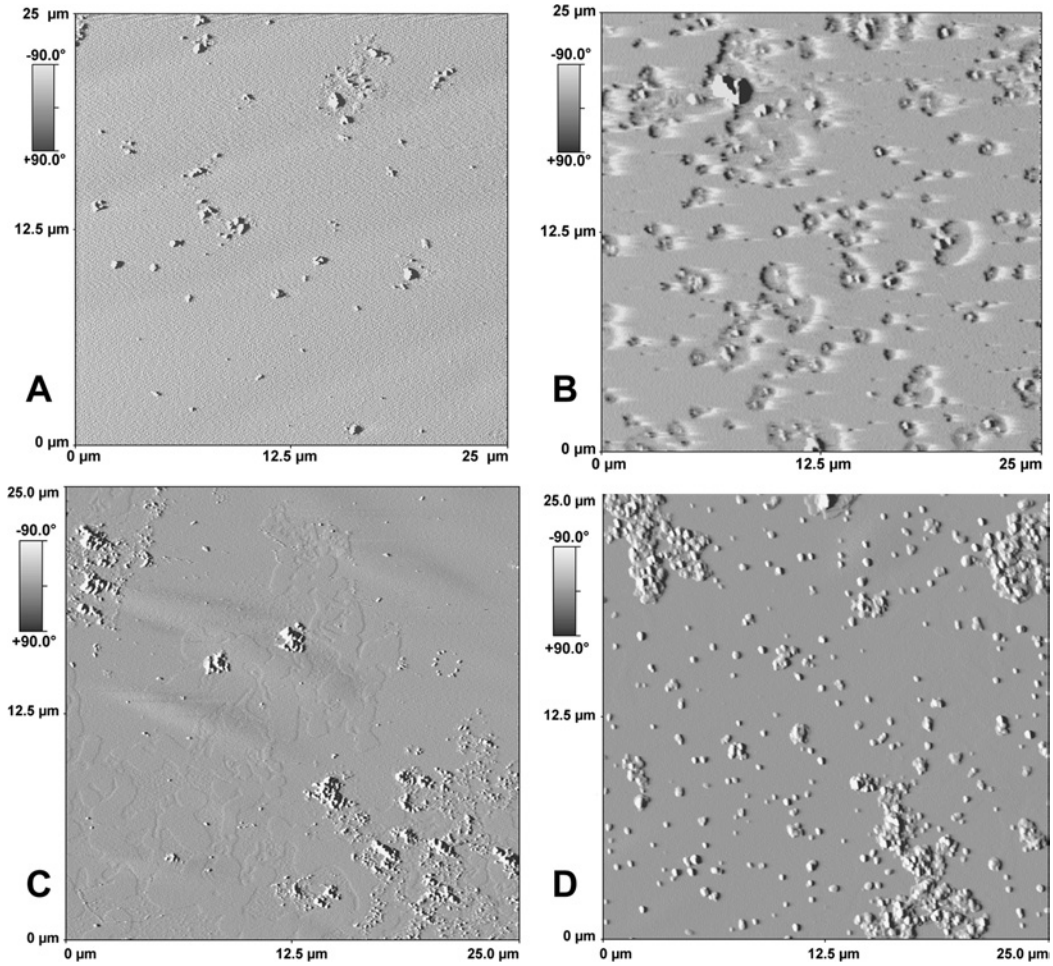

Figure 6 AFM imaging of DRM-enriched membrane bilayers

Non-treated, DRM-containing F3 fraction (**A**), and 40 % (**B**) or 60 % (**C**) cholesterol-depleted membranes and cholesterol-repleted membranes that had previously been depleted (**D**) were prepared as described in the Materials and methods section. After treatment and centrifugation, samples were sonicated for 3 × 30 s and 1–2.5 μg of proteins were deposited on a freshly cleaved mica plate before AFM analysis.

when compared with that of the non-treated fraction [121 nmol ATP · min^{-1} · (mg of protein)$^{-1}$], corresponds to a 52 % inhibition of the activity (Figure 5C). In addition, 90 % cholesterol repletion led to a major recovery of the P-gp ATPase activity in DRM-enriched fractions (Figures 5B and 5C). On the other hand, a depletion of 40 % cholesterol in fraction F7 did not provoke any alteration in the P-gp ATPase activity as for its repletion. However, the 104 % cholesterol overload of the non-treated fraction F7 (Figure 5D) caused a 58 % stimulation of the P-gp ATPase activity (Figure 5E); this value is highly significant considering the fact that P-gp is not the most representative protein in this fraction. Cholesterol saturation of the non-treated, DRM-containing fraction F3 did not exceed 21 % (Figure 3B) and did not modify significantly the P-gp ATPase activity (Figure 3C), suggesting that membrane cholesterol in fraction F3 was already close to saturation.

Effect of MβCD-induced cholesterol depletion as observed by AFM

AFM was used to show how cholesterol depletion and repletion modified the structure of biological membranes. AFM has been rarely used to study biological membrane models because of their heterogeneity and complexity. Figure 6(A) shows that the surface of control (non-treated) DRMs was homogeneous and the roughness was low (RMS = 2 nm). When DRM were incubated with MβCD, approx. 40–60 % of the total cholesterol was depleted, thus revealing two different behaviours. When 40 % depletion was achieved, Figure 6(B) shows that cholesterol depletion affected only the close region surrounding the proteins, which corresponded mostly to P-gp, as shown in Figure 7. Figure 6(B)

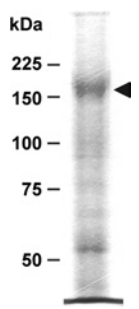

Figure 7 P-gp as revealed by electrophoresis of DRM-containing fraction

Proteins (10 μg) from fraction F3 were deposited on an SDS/8 % polyacrylamide gel and run as described in the Materials and methods section. The gel was stained with Coomassie Blue. The arrowhead points to the band corresponding to P-gp.

shows several patch-like depressions that form 1–1.5 μm diameter holes in the membrane, in the centre of which proteins protrude. In addition, Figure 6(B) shows that approx. 40 % cholesterol depletion did not induce protein aggregation. On the other hand, as shown in Figure 6(C), approx. 60 % cholesterol depletion stimulated protein aggregation and the apparition all around the protein of two phases, one of which protruded slightly from the background of the other by approx. 1.01–1.58 nm with an average of 1.22 nm obtained after 10 analyses; a majority of protein particles were apart from the relief, which corresponds to the remaining cholesterol-enriched domains. Cholesterol repletion of DRMs, inducing a roughness of 5.5 nm, was almost total in both cases and Figure 6(D) shows that cholesterol was reinserted into the regions that were previously depleted; however, the region surrounding the proteins seems to acquire a different organization without retrieving the roughness of the untreated fraction F3.

DISCUSSION

Chemoresistant cancer cells that express the typical MDR phenotype overproduce ABC transporters such as P-gp. Several reports have discussed the membrane protein–lipid changes related to this phenotype and, in particular, increased cholesterol [31] and glycosphingolipid [32] content, with the probable localization of P-gp to DRM regions and more particularly to caveolae [20,33]. Such lipid regions may specifically constrain P-gp into optimal environmental and functional conditions, which have not yet been fully documented. The present study clearly shows that in MDR cancer cells that express P-gp, two P-gp populations exist according to the presence or absence of closely surrounding cholesterol. One P-gp population with the highest P-gp ATPase activity is mostly found in the DRM-containing membrane fraction from chemoresistant CEM cells, the other population with the lowest P-gp ATPase activity is located elsewhere in the membrane. In addition, DRMs show a particular proteo-lipidic organization, which could not be retrieved by cholesterol repletion following their initial depletion.

Distribution of cholesterol and P-gp in membranes from CEM/VLB5 chemoresistant cells

With the modified DRM purification procedure described in the Materials and methods section, we found that the Triton X-100-insoluble and milky band in the 15–25 % sucrose fraction labelled F3, actually contains DRMs. Moreover, we co-detected P-gp and caveolin-1 in this fraction, suggesting that F3 contains DRMs, caveolae and P-gp. We have also found detectable amounts of P-gp in fractions F2, F4 and F5, which, as intermediate fractions, probably correspond to DRM diffusion. Since P-gp is barely detectable in the fraction F7, we conclude that this protein is mainly present in the cholesterol-rich membrane fractions. Co-detection of P-gp and caveolin-1 has already been reported and a possible interaction between caveolin-1 or caveolin-2 and P-gp has been suggested [18].

Distribution of active P-gp in membrane fractions from chemoresistant cells

The highest measured P-gp ATPase activity was found in the DRM-containing fractions for both moderately and highly resistant cells. This activity reached 144 nmol ATP $\cdot$ min^{-1} $\cdot$ (mg of total membrane proteins)$^{-1}$, which is within the range already reported by us and others for overall membrane P-gp ATPase activity [15]. Moreover, this activity is specific to P-gp since (i) in the presence of 200 μM of the P-gp-specific inhibitor orthovanadate, the P-gp ATPase activity in fraction F3 is almost totally inhibited and (ii) in the presence of the P-gp-specific verapamil regulator, the P-gp ATPase activity in fraction F3 is activated 2.8-fold for CEM/VLB5 cells.

Verapamil, which is a known specific P-gp activator, presented unexpectedly opposite effects when DRMs or soluble-membrane fractions were considered. We and others had previously reported that, on intact membranes from resistant CEM cells, verapamil in the same concentration range as that used for the present study activated the P-gp ATPase activity, whereas higher concentrations became progressively inhibitory [15]. The behaviour of P-gp ATPase activity as a function of verapamil concentration in cholesterol-depleted (40 %) or -saturated (100 %) DRM-containing (F3) or solubilized membrane (F7) fractions evolved according to a biphasic curve (Figure 3), whose mathematical model was very similar to that obtained with total membrane preparations. In the latter case, the curve obtained probably results from a combined effect due to the total P-gp ATPase activity in both DRMs and other membrane regions. The decreasing portion of the biphasic curve would be related to a P-gp ATPase activity, which could be inhibited by verapamil in fraction F7, and whose functioning, in terms of sensitivity to verapamil, differs from that observed in fraction F3, probably because of its different lipid microenvironment. However, we cannot exclude the possibility that the curve in Figure 3(C) is also biphasic, especially if the lack of cholesterol induces a shift in the maximum P-gp ATPase activation to the low verapamil concentrations as suggested by curves in Figures 3(A), 3(D) and 3(E). This idea is strengthened by a similar observation concerning P-gp reconstituted in liposomes with variable cholesterol concentration in the CH^{r}B30 cell line [34]. Consequently, it appears that cholesterol influences the verapamil-modulated P-gp ATPase activity; in addition, variation of cholesterol amounts may disturb the P-gp–drug interaction through the consecutive biochemical changes of the membrane. In any case, this effect may not be due to cholesterol but is rather the result of the P-gp close-membrane environment reorganization caused by the variation of cholesterol amounts [34]. In the same way, it was also proposed that the membrane lipid-phase state could affect ATP binding and hydrolysis by P-gp, but contrary to the previous statement, modulation of the P-gp ATPase activity can be caused by altered interactions between cholesterol or other lipids and transmembrane regions, or between nucleotide binding domains and the membrane surface [35]. The opposite behaviour observed for verapamil-modulated P-gp ATPase activity in fractions F3 and F7 strongly suggests that two P-gp populations exist in MDR cancer cells, as previously hypothesized [20]. These two P-gp populations may be characterized by different close microenvironments in which one of the membrane compounds involved is cholesterol. Concerning other MDR-related ABC transporters, it is interesting to notice that P-gp modulators do not induce the same effect depending on the ABC transporter considered. This could mean that ABC transporters do not have identical closed microenvironments, which leads to different protein–drug interactions as well as to different patterns of P-gp ATPase activity modulation [36].

The fact that the $A_{\Delta\psi} - A_{\pi}$ difference measured by the Langmuir method revealed a stabilizing effect of verapamil on the P-gp–lipid complexes, suggests first a direct interaction of verapamil with the membrane monolayer and secondly that lipids in the close P-gp microenvironment did not change when the membrane monolayer was formed. To support this idea, we had previously shown that to reconstitute purified P-gp in liposomes, it was necessary to peel off the tightly bound lipids, which invariably accompanied P-gp throughout the purification process, with a strong detergent such as SDS [37]; this does not exclude the possibility that the tightly bound lipids may differ in P-gp located in DRMs compared with

P-gp located elsewhere, while these lipids remain strongly bound to P-gp of both populations. It should be noted that the result reported in Figure 4 shows the overall effect of verapamil on membrane monolayers from CEM/VLB0.45 cells. Our results suggest that the P-gp population in fraction F3 could be associated with particular lipids of DRM regions, which confer on P-gp its P-gp ATPase activity and which can be activated by verapamil. In contrast, the verapamil-induced inhibition of P-gp ATPase activity in fraction F7 suggests that (i) lipids in the close P-gp microenvironment are of a different nature so that they do not promote a functional stabilization of P-gp–lipid complexes and/or (ii) the Triton X-100-induced membrane disruption could have sensitized the P-gp ATPase activity due to its inhibition by verapamil. In this latter case, we can exclude a possible inhibitory effect of Triton X-100 on the P-gp ATPase activity in fraction F7, since the total P-gp ATPase activity in crude membrane extracts before any treatment was barely higher than that of the summed total P-gp ATPase activities measured in each fraction. Moreover, due to the large amount of protein in fraction F7, one can imagine that the inhibitory effect of verapamil could be related to another ATPase activity. However, in fraction F7, at least 60 % of the activity is actually due to P-gp since it could be inhibited by orthovanadate.

Role of cholesterol in the activation of P-gp ATPase activity and evidence for the existence of two P-gp populations

Results of the present study and also those of others showed that P-gp was localized mostly in DRMs, the remaining P-gp molecules being located in soluble membranes in quantities depending on the cell line [20,38]. However, the close microenvironment surrounding P-gp in these two regions is still unknown. Our results show that P-gp is surrounded by cholesterol, which directly affects P-gp ATPase activity when it is removed from the membrane environment. It has been previously reported that detergent-purified P-gp retains some lipids [39] and that certain lipids surrounding P-gp that was reconstituted in liposomes can influence its P-gp ATPase activity [14]. In addition, drugs that affect the P-gp-surrounding lipids change its P-gp ATPase activity [13]. Conversely, it has been reported that membrane fluidization induces a modulation of the P-gp ATPase activity [40]. Our results show that depletion of cholesterol in DRM-enriched fractions induced a decreased P-gp ATPase activity, whereas its repletion allowed an almost complete recovery of the original P-gp ATPase activity. Although approx. 50 % cholesterol depletion results in a comparable approx. 50 % decrease in P-gp ATPase activity, we can conclude that the residual ATPase activity is also influenced by the fraction of cholesterol that was not extracted from fraction F3 since we reported elsewhere that membrane cholesterol amounts and P-gp ATPase activity are linked by a linear relationship [41]. On the contrary, in fraction F7, neither 40 % cholesterol depletion nor its repletion caused any modulation of the P-gp ATPase activity. We can suppose that the amount of cholesterol surrounding P-gp is too low or absent to observe a measurable alteration of the P-gp ATPase activity.

Attempts to saturate DRMs with cholesterol failed to exceed 21 % of the initial cholesterol amount, whereas the level of cholesterol saturation of the solubilized-membrane-containing fraction could reach 104 %, suggesting that the latter was completely saturated with cholesterol. In addition, the 21 % cholesterol overload did not have any effect on the P-gp ATPase activity. On the contrary, the cholesterol amount in fraction F7 was initially much lower than that of fraction F3 so that cholesterol saturation caused a 58 % stimulation of the P-gp ATPase activity. Thus, cholesterol appears as a sufficient element to modify this activity. Although the role of cholesterol in P-gp ATPase activity was already described in several membrane models, it appears that some information concerning the precise role of DRMs in the stimulation of P-gp ATPase activity is missing. Thus, DRMs constitute an environment in which P-gp can display an optimal P-gp ATPase activity.

Our results suggest that two different populations of P-gp are present in the membranes of MDR cancer cells. One population, which is localized in the DRM regions, has the highest proportion of P-gp molecules in a cholesterol-rich membrane environment and displays an optimal P-gp ATPase activity. It should be mentioned however that a fraction of the initial activity may be inhibited by the proximity of P-gp with caveolin-1, as suggested by a recent study concerning caveolar microdomains of an *in vitro* model of the blood–brain barrier, in which caveolin-1 decreases the transport activity of P-gp [18]. The second population has a low proportion of P-gp molecules in a cholesterol-poor environment and is localized elsewhere in the membrane. In addition, this population is characterized by approx. 8.3-fold lower P-gp ATPase activity.

Visualization of cholesterol depletion by AFM

Our AFM results showed that in the biological DRM-rich membranes from fraction F3, cholesterol depletion induces the disappearance of raft-like structures and shows the appearance of relief corresponding to the remaining DRMs. We have thus evidenced the fact that depletion of cholesterol in a cholesterol-rich membrane domain caused the disruption of ordered liquid phase, and the remaining DRMs appear as a layer with a thickness of approx. 1.01–1.58 nm. This value, which is close to that reported for AFM of cholesterol-enriched domains that have a height difference of 1.4 nm from the rest of the membrane [42], corresponds to the difference in length between cholesterol and phospholipids in reconstituted membranes. This is the first time that both DRMs and the effect of their cholesterol depletion are observed by AFM on biological membrane extracts.

MβCD affects primarily the P-gp close microenvironment. It has been suggested that P-gp could locally destabilize the membrane [34]. This hypothesis could explain why cholesterol is first depleted in its close microenvironment, because this region may be less stable than others. In addition, the region in which P-gp is embedded seems to be highly enriched in cholesterol, thus providing new evidence about the role of cholesterol in P-gp structuring. Conversely, P-gp shows a high propensity to sequester in cholesterol-rich membrane regions; this may be a general feature that concerns several proteins as reported in a recent review [43]. The high P-gp ATPase activity of P-gp sequestered in these domains is evidence of their biological importance in creating a functional environment for P-gp.

When a cholesterol depletion of 40 % was achieved, P-gp lost its P-gp ATPase activity even if the whole membrane maintained its organization, in contrast to what occurs with 60 % cholesterol depletion. During its repletion, cholesterol is preferentially inserted into the depleted regions. Since in this case P-gp ATPase activity is recovered, this means that its activation requires close cholesterol. However, AFM results show that the microenvironment close to P-gp remains altered. This may be due to the particular structure of MβCD-loaded cholesterol, which could provoke perturbation in the membrane organization.

In conclusion, after cholesterol depletion, AFM results show that no proteins remain in the DRM regions, indicating that P-gp has been translocated to non-DRM regions. After cholesterol repletion, P-gp is reinserted into DRMs where it recovers its P-gp ATPase activity. Thus, cholesterol appears to be an essential component of DRMs for maintaining the structure of P-gp, which

is compatible with its optimal activity. The intimate interaction between P-gp and cholesterol still remains unknown. However, in view of all the results obtained, cholesterol appears as a new potential therapeutic target to fight the typical MDR phenotype.

This work was supported by grants from the Ligue contre le Cancer: Comité de la Loire, Comité de la Drôme, the Fondation pour la Recherche Médicale and the Fondation Mérieux. G.D. thanks the Ligue contre le Cancer: Comité National and Comité du Rhône, and A.L. thanks Delta Proteomics for financial support.

REFERENCES

1 Gottesman, M. M. (1993) How cancer cells evade chemotherapy: sixteenth Richard and Hinda Rosenthal Foundation Award Lecture. Cancer Res. **53**, 747–754
2 Hamada, H. and Tsuruo, T. (1988) Purification of the 170- to 180-kilodalton membrane glycoprotein associated with multidrug resistance. 170- to 180-kilodalton membrane glycoprotein is an ATPase. J. Biol. Chem. **263**, 1454–1458
3 Demeule, M., Jodoin, J., Gingras, D. and Beliveau, R. (2000) P-glycoprotein is localized in caveolae in resistant cells and in brain capillaries. FEBS Lett. **466**, 219–224
4 Fujimoto, T. (1996) GPI-anchored proteins, glycosphingolipids, and sphingomyelin are sequestered to caveolae only after crosslinking. J. Histochem. Cytochem. **44**, 929–941
5 Fujimoto, T., Hayashi, M., Iwamoto, M. and Ohno-Iwashita, Y. (1997) Crosslinked plasmalemmal cholesterol is sequestered to caveolae: analysis with a new cytochemical probe. J. Histochem. Cytochem. **45**, 1197–1205
6 Lisanti, M. P., Tang, Z. L. and Sargiacomo, M. (1993) Caveolin forms a hetero-oligomeric protein complex that interacts with an apical GPI-linked protein: implications for the biogenesis of caveolae. J. Cell Biol. **123**, 595–604
7 Rothberg, K. G., Heuser, J. E., Donzell, W. C., Ying, Y. S., Glenney, J. R. and Anderson, R. G. (1992) Caveolin, a protein component of caveolae membrane coats. Cell (Cambridge, Mass.) **68**, 673–682
8 Ahmed, S. N., Brown, D. A. and London, E. (1997) On the origin of sphingolipid/cholesterol-rich detergent-insoluble cell membranes: physiological concentrations of cholesterol and sphingolipid induce formation of a detergent-insoluble, liquid-ordered lipid phase in model membranes. Biochemistry **36**, 10944–10953
9 Lisanti, M. P., Scherer, P. E., Vidugiriene, J., Tang, Z., Hermanowski-Vosatka, A., Tu, Y. H., Cook, R. F. and Sargiacomo, M. (1994) Characterization of caveolin-rich membrane domains isolated from an endothelial-rich source: implications for human disease. J. Cell Biol. **126**, 111–126
10 Arsenault, A. L., Ling, V. and Kartner, N. (1988) Altered plasma membrane ultrastructure in multidrug-resistant cells. Biochim. Biophys. Acta **938**, 315–321
11 Garcia-Segura, L. M., Ferragut, J. A., Ferrer-Montiel, A. V., Escriba, P. V. and Gonzalez-Ros, J. M. (1990) Ultrastructural alterations in plasma membranes from drug-resistant P388 murine leukemia cells. Biochim. Biophys. Acta **1029**, 191–195
12 Lavie, Y., Fiucci, G., Czarny, M. and Liscovitch, M. (1999) Changes in membrane microdomains and caveolae constituents in multidrug-resistant cancer cells. Lipids **34 (Suppl.)**, S57–S63
13 Urbatsch, I. L. and Senior, A. E. (1995) Effects of lipids on ATPase activity of purified Chinese hamster P-glycoprotein. Arch. Biochem. Biophys. **316**, 135–140
14 Sharom, F. J. (1997) The P-glycoprotein multidrug transporter: interactions with membrane lipids, and their modulation of activity. Biochem. Soc. Trans. **25**, 1088–1096
15 Dong, M., Penin, F. and Baggetto, L. G. (1996) Efficient purification and reconstitution of P-glycoprotein for functional and structural studies. J. Biol. Chem. **271**, 28875–28883
16 Garrigues, A., Escargueil, A. E. and Orlowski, S. (2002) The multidrug transporter, P-glycoprotein, actively mediates cholesterol redistribution in the cell membrane. Proc. Natl. Acad. Sci. U.S.A. **99**, 10347–10352
17 Hinrichs, J. W., Klappe, K., Hummel, I. and Kok, J. W. (2004) ATP-binding cassette transporters are enriched in non-caveolar detergent-insoluble glycosphingolipid-enriched membrane domains (DIGs) in human multidrug-resistant cancer cells. J. Biol. Chem. **279**, 5734–5738
18 Jodoin, J., Demeule, M., Fenart, L., Cecchelli, R., Farmer, S., Linton, K. J., Higgins, C. F. and Beliveau, R. (2003) P-glycoprotein in blood-brain barrier endothelial cells: interaction and oligomerization with caveolins. J. Neurochem. **87**, 1010–1023
19 Troost, J., Albermann, N., Emil Haefeli, W. and Weiss, J. (2004) Cholesterol modulates P-glycoprotein activity in human peripheral blood mononuclear cells. Biochem. Biophys. Res. Commun. **316**, 705–711
20 Lavie, Y., Fiucci, G. and Liscovitch, M. (1998) Up-regulation of caveolae and caveolar constituents in multidrug-resistant cancer cells. J. Biol. Chem. **273**, 32380–32383
21 Luker, G. D., Pica, C. M., Kumar, A. S., Covey, D. F. and Piwnica-Worms, D. (2000) Effects of cholesterol and enantiomeric cholesterol on P-glycoprotein localization and function in low-density membrane domains. Biochemistry **39**, 7651–7661
22 Modok, S., Heyward, C. and Callaghan, R. (2004) P-glycoprotein retains function when reconstituted into a sphingolipid- and cholesterol-rich environment. J. Lipid Res. **45**, 1910–1918
23 Baggetto, L. G., Dong, M., Bernaud, J., Espinosa, L., Rigal, D., Bonvallet, R. and Marthinet, E. (1998) *In vitro* and *in vivo* reversal of cancer cell multidrug resistance by the semi-synthetic antibiotic tiamulin. Biochem. Pharmacol. **56**, 1219–1228
24 Bradford, M. M. (1976) A rapid and sensitive method for the quantitation of microgram quantities of protein utilizing the principle of protein-dye binding. Anal. Biochem. **72**, 248–254
25 Heider, J. G. and Boyett, R. L. (1978) The picomole determination of free and total cholesterol in cells in culture. J. Lipid Res. **19**, 514–518
26 Allain, C. C., Poon, L. S., Chan, C. S., Richmond, W. and Fu, P. C. (1974) Enzymatic determination of total serum cholesterol. Clin. Chem. **20**, 470–475
27 Nakamura, M., Kondo, H., Shimada, Y., Waheed, A. A. and Ohno-Iwashita, Y. (2003) Cellular aging-dependent decrease in cholesterol in membrane microdomains of human diploid fibroblasts. Exp. Cell Res. **290**, 381–390
28 Zaitsev, S., Volchenkova, T. A., Ustinova, O. A., Koshtigo, T. V., Bagetto, L. G., Fleury, F., Madoulet, S., Nabiev, I. R. and Oleinikov, V. A. (2002) Study of P-glycoprotein effect on the lipid monolayer properties by the Langmuir-Blodgett technique. Biofizika **47**, 1073–1079 (in Russian)
29 Okamoto, T., Schlegel, A., Scherer, P. E. and Lisanti, M. P. (1998) Caveolins, a family of scaffolding proteins for organizing 'preassembled signaling complexes' at the plasma membrane. J. Biol. Chem. **273**, 5419–5422
30 Garrigues, A., Loiseau, N., Delaforge, M., Ferte, J., Garrigos, M., Andre, F. and Orlowski, S. (2002) Characterization of two pharmacophores on the multidrug transporter P-glycoprotein. Mol. Pharmacol. **62**, 1288–1298
31 May, G. L., Wright, L. C., Dyne, M., Mackinnon, W. B., Fox, R. M. and Mountford, C. E. (1988) Plasma membrane lipid composition of vinblastine sensitive and resistant human leukaemic lymphoblasts. Int. J. Cancer **42**, 728–733
32 Lavie, Y., Cao, H., Bursten, S. L., Giuliano, A. E. and Cabot, M. C. (1996) Accumulation of glucosylceramides in multidrug-resistant cancer cells. J. Biol. Chem. **271**, 19530–19536
33 Virgintino, D., Robertson, D., Errede, M., Benagiano, V., Girolamo, F., Maiorano, E., Roncali, L. and Bertossi, M. (2002) Expression of P-glycoprotein in human cerebral cortex microvessels. J. Histochem. Cytochem. **50**, 1671–1676
34 Rothnie, A., Theron, D., Soceneantu, L., Martin, C., Traikia, M., Berridge, G., Higgins, C. F., Devaux, P. F. and Callaghan, R. (2001) The importance of cholesterol in maintenance of P-glycoprotein activity and its membrane perturbing influence. Eur. Biophys. J. **30**, 430–442
35 Romsicki, Y. and Sharom, F. J. (1998) The ATPase and ATP-binding functions of P-glycoprotein – modulation by interaction with defined phospholipids. Eur. J. Biochem. **256**, 170–178
36 Cole, S. P., Sparks, K. E., Fraser, K., Loe, D. W., Grant, C. E., Wilson, G. M. and Deeley, R. G. (1994) Pharmacological characterization of multidrug resistant MRP-transfected human tumor cells. Cancer Res. **54**, 5902–5910
37 Dong, M., Baggetto, L. G., Falson, P., Le Maire, M. and Penin, F. (1997) Complete removal and exchange of sodium dodecyl sulfate bound to soluble and membrane proteins and restoration of their activities, using ceramic hydroxyapatite chromatography. Anal. Biochem. **247**, 333–341
38 Yang, C. P., Galbiati, F., Volonte, D., Horwitz, S. B. and Lisanti, M. P. (1998) Upregulation of caveolin-1 and caveolae organelles in Taxol-resistant A549 cells. FEBS Lett. **439**, 368–372
39 Sharom, F. J., Yu, X., Chu, J. W. and Doige, C. A. (1995) Characterization of the ATPase activity of P-glycoprotein from multidrug-resistant Chinese hamster ovary cells. Biochem. J. **308**, 381–390
40 Regev, R., Assaraf, Y. G. and Eytan, G. D. (1999) Membrane fluidization by ether, other anesthetics, and certain agents abolishes P-glycoprotein ATPase activity and modulates efflux from multidrug-resistant cells. Eur. J. Biochem. **259**, 18–24
41 Gayet, L., Dayan, D., Barakat, S., Labialle, S., Michaud, M., Cogne, S., Mazane, A., Coleman, A. W., Rigal, D. and Baggetto, L. G. (2005) Control of P-glycoprotein activity by membrane cholesterol amounts and their relation to multidrug resistance, in human CEM leukemia cells. Biochemistry **44**, 4499–4509
42 Tokumasu, F., Jin, A. J., Feigenson, G. W. and Dvorak, J. A. (2003) Nanoscopic lipid domain dynamics revealed by atomic force microscopy. Biophys. J. **84**, 2609–2618
43 Epand, R. M. (2004) Do proteins facilitate the formation of cholesterol-rich domains? Biochim. Biophys. Acta **1666**, 227–238

Received 2 December 2004/4 January 2005; accepted 7 February 2005
Published as BJ Immediate Publication 7 February 2005, DOI 10.1042/BJ20041999